Invited Paper

Terahertz solid immersion microscopy for sub-wavelength-resolution imaging of biological objects and tissues

Nikita V. Chernomyrdin[a], Anna S. Kucheryavenko[a], Kirill M. Malakhov[a], Alexander O. Schadko[a], Gennady A. Komandin[b], Sergey P. Lebedev[b], Irina N. Dolganova[a], Vladimir N. Kurlov[c], Denis V. Lavrukhin[d], Dmitry S. Ponomarev[d], Stanislav O. Yurchenko[a], Valery V. Tuchin[e,f,g], and Kirill I. Zaytsev[a,b]

[a]Bauman Moscow State Technical University, Moscow 105005, Russia
[b]A.M. Prokhorov General Physics Institute of RAS, Moscow 119991, Russia
[c]Institute of Solid State Physics of RAS, Chernogolovka 142432, Russia
[d]Institute of Ultra High Frequency Semiconductor Electronics of RAS, Moscow 117105, Russia
[e]Saratov State University, Saratov 410012, Russia
[f]Institute of Precision Mechanics and Control of RAS, Saratov 410028, Russia
[g]Tomsk State University, Tomsk 634050, Russia

ABSTRACT

We have developed a method of terahertz (THz) solid immersion microscopy for imaging of biological objects and tissues. It relies on the solid immersion lens (SIL) employing the THz beam focusing into the evanescent-field volume and allowing strong reduction in the dimensions of the THz beam caustic. By solving the problems of the sample handling at the focal plane and raster scanning of its surface with the focused THz beam, the THz SIL microscopy has been adapted for imaging of soft tissues. We have assembled an experimental setup based on a backward-wave oscillator, as a continuous-wave source operating at the wavelength of $\lambda = 500$ μm, and a Golay cell, as a detector of the THz wave intensity. By imaging of the razor blade, we have demonstrated advanced 0.2λ-resolution of the proposed THz SIL configuration. Using the experimental setup, we have performed THz imaging of a mint leaf revealing its sub-wavelength features. The observed results highlight a potential of the THz SIL microscopy in biomedical applications of THz science and technology.

Keywords: terahertz imaging, solid immersion lens, solid immersion microscopy, sub-wavelength resolution, biological tissues

1. INTRODUCTION

Methods of 2D[1,2] and 3D[3,4] terahertz (THz) imaging have been vigorously explored during the past decades. Nowadays, they offer scientific and technological applications in biology and medicine,[5] non-destructive sensing[6,7] and security tasks,[8–10] chemical[11] and pharmaceutical[12] industries. Despite the considerable progress in the THz imaging technologies, a practical reliability of the majority of the THz imaging systems is significantly limited by their low spatial resolution.[13] Achieving sub-wavelength spatial resolution of THz imaging remains one of the key problems of THz science and technology. This problem is of particular importance for rapidly developing THz biomedicine,[14] since the components of biological objects and tissues have essentially sub-wavelength scale compared to the THz wavelengths.[15–18]

Several approaches for bringing the THz imaging resolution to sub-wavelength scales have been recently developed relying on various physical phenomena. Let us briefly discuss these developments considering the Rayleigh criterion of imaging resolution,[19,20] which states that two points of equal intensity should be considered

Further author information: Send correspondence to
Nikita V. Chernomyrdin, E-mail: chernik-a@yandex.ru and Kirill I. Zaytsev, E-mail: kirzay@gmail.com

Saratov Fall Meeting 2017: Optical Technologies in Biophysics and Medicine XIX, edited by Elina A. Genina, Irina Yu. Goryacheva. Valery V. Tuchin, Proc. of SPIE Vol. 10716, 1071606
 · doi: 10.1117/12.2314464

to be resolved in case of the principal intensity maximum of one coincides with the first intensity minimum of the other (or, when one beam spot is spaced on an Airy disc radius from the other). Most of the modern applications of THz imaging and spectroscopy are based on the use of single element optical systems – wide aperture spherical and aspherical lenses, or off-axis parabolic mirrors,[13] which yield reduction of the THz beam spot radius to 0.8...1.0λ, where λ is an electromagnetic wavelength. Further improvement of performance of the single element optics by increasing numerical aperture and resolution seems to be challenging owing to the residual wavefront aberrations, inherent to lenses,[21] or overlapping of incident and focused beams, inherent to the off-axis parabolic mirrors.[13] Recently, several methods of THz imaging with the resolution beyond the $\lambda/2$ Abbe limit have been proposed relying on the lens-based optical systems and exploiting the effects of electromagnetic field localization behind mesoscale obstacles or particles placed in front of the focal plane.[22] Among them are the THz solid immersion imaging[23,24] and the THz imaging based on optical jets.[25] These methods yield slightly sub-wavelength spatial resolution. However, they seem to be sub-optimal for THz imaging of biological objects and tissues owing to the technical difficulties of soft samples' handling at the focal plane and raster scanning of their surface by the THz beam caustic possessing very small depth of field.[24]

THz digital holography[26] and synthetic aperture imaging[27] represent other modalities of THz imaging, which are capable for lens-less operation. The spatial resolution of these methods could reach slightly sub-wavelength scales. However, these methods require complicated computations for accurate resolving the inverse ill-posed problems,[28–30] the solution of which could be rather unstable in case of studying the objects with complex shape. Various methods of THz near-field imaging[31] allow for overcoming the diffraction limit and achieving essentially sub-wavelength resolution of 0.1λ, and even 0.001λ.[32,33] While providing superior spatial resolution, the near-field imaging techniques are plagued with many drawbacks. They require small working distance, thus, the scanning probe placed at the object plane may interact with the object. Detection of light scattered by the small scanning probe requires powerful emitters and sensitive detectors,[34] which are still rare and expensive.[35] The THz near-field imaging has been recently applied for studying tissues.[36] Nevertheless, it is still a laborious instrument, which is hardly-reliable in clinical practice.

In this paper, we propose a novel arrangement of the THz solid immersion microscopy, which yields imaging of biological objects and tissues. The THz solid immersion microscopy relies on the use of so-called solid immersion lens (SIL),[24] which employs the THz beam focusing into the evanescent-field volume and allows for strong reduction in the dimensions of the THz beam caustic. We solve the problems of the sample handling at the focal plane and raster scanning of its surface by the focused THz beam, which makes possible using the THz SIL microscopy for studying soft biological object and tissues. We assemble an experimental setup, which realizes the proposed configuration of the THz SIL microscopy and includes a backward-wave oscillator as a continuous-wave source with the output wavelength of $\lambda = 500$ μm, and a Golay cell as a detector of the THz field intensity. We experimentally demonstrate advanced 0.2λ-resolution of the THz SIL microscope. Finally, we apply it for imaging of a representative biological tissue – a mint leaf. The observed results reveal sub-wavelength features of the sample justifying prospectives of the THz SIL microscopy in biomedical technologies.

2. EXPERIMENTAL SETUP

We assembled an experimental setup realizing the proposed configuration of the THz SIL microscopy. Figure 1 shows (a) a scheme of this setup and (b) a separate scheme illustrating details of the THz SIL construction. From the Fig. 1 (a), we could notice that the setup is quite similar to the ones employed in earlier papers[21,24] – it uses the principles of a raster-scan continuous-wave THz imaging in reflection mode. As a source of continuous-wave THz radiation with the wavelength of $\lambda = 500$ μm, we used a backward-wave oscillator.[37] As a THz wave detector, we used a Golay cell.[38] A 22 Hz mechanical chopper was employed for the THz beam modulation, since the Golay cell is capable for detecting only the modulated intensity of electromagnetic field. Furthermore, an attenuator was applied for preventing the overload of the detector. We homogenized an intensity in the cross-section of the THz beam by its passing through a 1-mm-diameter metal diaphragm. We employed a high-resistivity float-zone silicon (HRFZ-Si) beamsplitter to realize the reflection-mode configuration of measurements with the normal angle of the THz beam incidence on a sample surface.

From the Fig. 1 (b), we could notice that the developed THz SIL is comprized of three optical elements – the wide-aperture aspherical singlet made of high-density polyethylene (HDPE), sphere and window made from

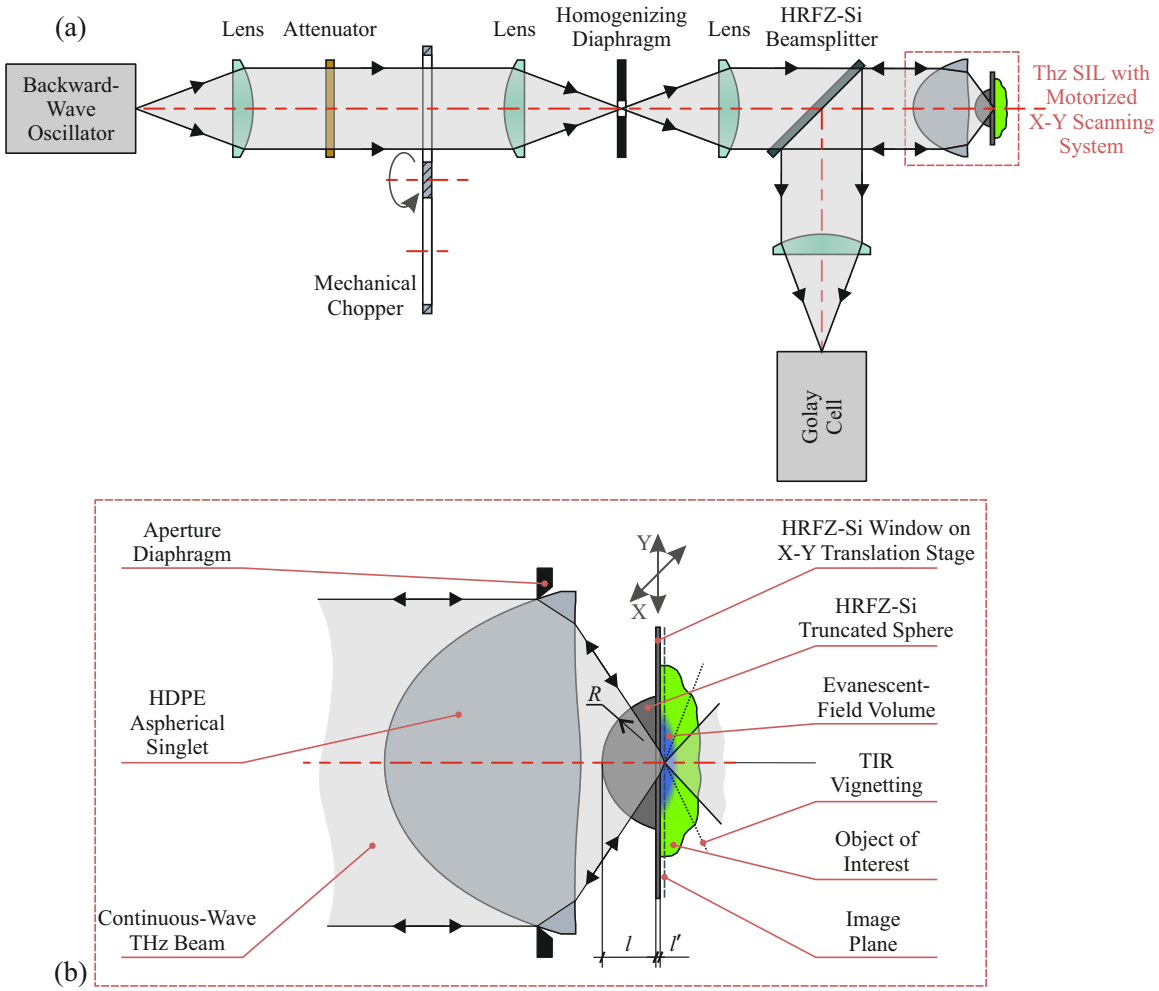

Figure 1. An experimental setup realizing the proposed configuration of the THz SIL microscopy: (a) a scheme of the setup, in general; (b) a scheme of the THz SIL comprised of a rigidly-fixed HDPE aspherical singlet, a rigidly-fixed HRFZ-Si truncated sphere, and a movable HRFZ-Si window. Being placed in a close contact with the rigidly-fixed HRFZ-Si truncated sphere, the movable HRFZ-Si window serves (i) as a part of the unitary optical element (i.e. a resolution enhancing hemisphere) and (ii) as a reference movable window allowing to handle a soft tissue sample during the raster scanning.

HRFZ-Si. The latter is mounted on motorized X-Y translation stage and allows for scanning the sample surface by the focused THz beam. The aspherical singlet possesses a focal length of $f' = 15$ mm, a numerical aperture of NA $= 0.64$, a back focal distance of $S'_{F'} = 6.62$ mm, an entrance pupil diameter of $D = 25.4$ mm, and a thickness of $t = 15$ mm.[21] The HRFZ-Si truncated sphere has a radius of $R = 10$ mm and a thickness of $l = 4.7$ mm.[24] Its spherical surface is concentric to the convergent THz wavefront, and its planar surface is parallel to the image plane. The HRFZ-Si window has a thickness of $l' = 0.25$ mm and a diameter of $\varnothing = 60$ mm, which is much larger compared to the dimensions of the truncated sphere, the THz beam caustic, and the sample of interest.

Being placed in a close contact with the rigidly-fixed HRFZ-Si truncated sphere, the movable HRFZ-Si window serves simultaneously as a part of unitary optical element (a hemisphere with a radius of $R = 10$ mm and a thickness of $l + l' = 4.95$ mm, which is placed in front of the focal plane for the resolution enhancement) and as a reference movable window allowing to handle soft samples and form their images via the raster scanning. Thus, this innovative configuration of the THz SIL makes possible microscopic imaging of biological objects and tissues. In order to satisfy the Whittaker–Nyquist–Kotelnikov–Shannon sampling theorem,[39] in experimental

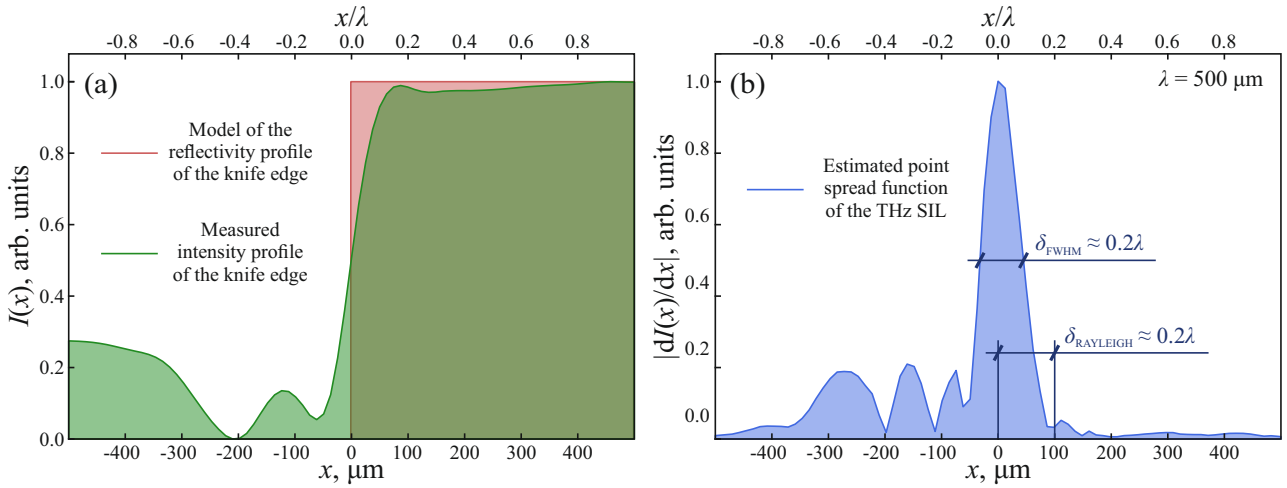

Figure 2. Estimation of the THz SIL microscopy resolution via the razor blade imaging: (a) a modeled step-function-like profile of the test-object reflectivity and a measured profile of the backscattered THz field intensity $I(x)$; (b) a THz beam spot estimation based on the razor blade imaging using the differentiation procedure $|dI(x)/dx|$.

study, we use a step of the raster scan of $0.1\lambda = 50$ μm, which is much larger compared to the 10-μm-accuracy of the X-Y translation stage positioning.

3. SPATIAL RESOLUTION OF THE THZ SIL MICROSCOPY

In order to examine the spatial resolution provided by the proposed configuration of the THz SIL microscopy, we used the described experimental setup for imaging of a razor blade – i.e. a convenient test object featuring a step-function-like (a Heaviside-functions-like[40]) spatial distribution of reflectivity.[41]

Figure 2 shows the results of razor blade imaging using the proposed THz SIL. Panel (a) illustrates both the modeled step-function-like profile of the test-object reflectivity and the measured profile of the backscattered THz field intensity $I(x)$. Panel (b) demonstrates a THz beam spot estimation based on the razor blade imaging using the differentiation procedure $|dI(x)/dx|$.[24,41] It is evident from Figure 2 that the THz SIL microscopy provides sharp image of the razor blade with strongly sub-wavelength resolution. Based on the data of Fig. 2 (b), we estimated a $\delta = 0.2\lambda$-resolution of the THz SIL microscopy according to both the Rayleigh resolution criterion[19,20] and the full-width at half-maximum (FWHM) of the THz beam spot.

Along with the advanced resolution, in Fig. 2 (b), we see oscillating and asymmetric character of the beam spot formed by the THz SIL. This peculiar geometry of the beam spot might originate from either an electromagnetic wave interference inside the HRFZ-Si hemisphere or some misalignments of the experimental setup, for instance, decentering of axes of the aspherical singlet and the truncated sphere. Meanwhile, these beam spot peculiarities do not significantly impact the estimated resolution of the THz SIL microscopy.

4. THZ SIL MICROSCOPY OF A MINT LEAF

Next, in order to highlight an ability of performing the THz SIL microscopy of biological objects and tissues, we applied the developed setup for imaging of a representative tissue – i.e. a mint leaf containing the sub-wavelength structural inhomogeneities. Figure 3 shows the results of the THz SIL microscopy of the mint leaf, where (a) and (b) demonstrate ordinary and magnified visual images of the leaf, and (c) presents its THz image (the imaged area is 4×4 mm^2 or $8 \times 8\lambda^2$).

In the THz image (Fig. 3 (c)), we clearly observed sub-wavelength features of the leaf with the scales larger than the estimated spatial resolution $\delta = 0.2\lambda$ of the THz SIL. Higher intensity of the back-scattered THz field is inherent to the veins and blade of the leaf, which might originate from both higher water content and density of the leaf's structural components.

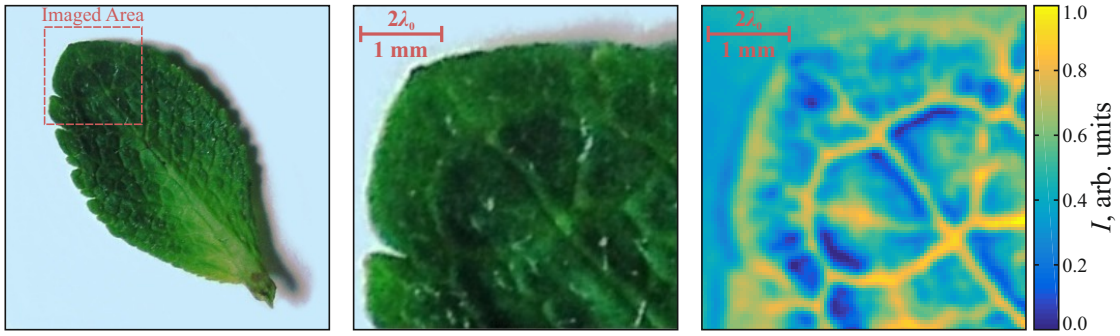

Figure 3. THz SIL microscopy of the mint leaf: (a),(b) ordinary and magnified visual images of the leaf, (c) its THz image. The area of THz image is $4 \times 4\text{-mm}^2$, or $8 \times 8\lambda^2$.

5. DISCUSSIONS

The proposed configuration of the THz SIL is beneficial from a favourable combination of a solid immersion phenomenon with a basic wide-aperture aspherical singlet.[21] The experimentally-estimated 0.2λ-resolution of this innovative THz SIL represents a considerable improvement over the earlier reported arrangements offering only 0.35λ-, 0.49λ- and 0.54λ-resolution.[24,42,43] The proposed THz SIL does not employ any sub-wavelength diaphragm (pinhole), thus, avoiding an undesirable losses of the THz wave intensity, which are common for the methods of near-field imaging.[31] Many standard THz lens-based imaging systems, including continuous-wave and pulsed ones, can be easily modified into the THz SIL configuration by simply placing the HRFZ-Si truncated sphere and the HRFZ-Si window in front of the focal plane.

Finally, the developed THz SIL microscopy operates in reflection mode providing an ability for *in vivo* imaging of non-transparent biological objects and tissues.[14] Thereby, the developed THz SIL microscopy could be applied for mapping the water content and the structural inhomogeneities of the sample. It has great potential in imaging of structurally-inhomogeneous solid-state materials,[44] discriminating pathological tissues from normal ones in medical diagnosis,[45–49] and detection of sub-wavelength-scale defects in constructional materials.[7]

6. CONCLUSIONS

In this work, we have proposed an innovative arrangement of the THz SIL microscopy, which yields imaging of soft samples. We have experimentally demonstrated advanced 0.2λ-resolution of the proposed THz SIL arrangement, as well as an ability of its use for imaging of biological objects and tissues.

ACKNOWLEDGMENTS

The work was supported by the Russian Science Foundation (RSF), Project # 17-79-20346.

REFERENCES

[1] Hu, B. and Nuss, M., "Imaging with terahertz waves," *Opt. Lett.* **20**(16), 1716–1718 (1995).

[2] Gregory, I., Tribe, W., Baker, C., Cole, B., Evans, M., Spencer, L., Pepper, M., and Missous, M., "Continuous-wave terahertz system with a 60 dB dynamic range," *Appl. Phys. Lett.* **86**(20), 204104 (2005).

[3] Mittleman, D. M., Hunsche, S., Boivin, L., and Nuss, M. C., "T-ray tomography," *Opt. Lett.* **22**(12), 904–906 (1997).

[4] Ferguson, B., Wang, S., Gray, D., Abbot, D., and Zhang, X.-C., "T-ray computed tomography," *Opt. Lett.* **27**(15), 1312–1314 (2002).

[5] Sun, Q., He, Y., Liu, K., Fan, S., Parrott, E., and Pickwell-MacPherson, E., "Recent advances in terahertz technology for biomedical applications," *Quantitative Imaging in Medicine and Surgery* **7**(3), 345–355 (2017).

[6] Kawase, K., Ogawa, Y., Watanabe, Y., and Inoue, H., "Non-destructive terahertz imaging of illicit drugs using spectral fingerprints," *Opt. Exp.* **11**(20), 2549–2554 (2003).

[7] Stoik, C., Bohn, M., and Blackshire, J., "Nondestructive evaluation of aircraft composites using transmissive terahertz time domain spectroscopy," *Opt. Exp.* **16**(21), 17039–17051 (2008).
[8] Grossman, E., Dietlein, C., Ala-Laurinaho, J., Leivo, M., Gronberg, L., Gronholm, M., Lappalainen, P., Rautiainen, A., Tamminen, A., and Luukanen, A., "Passive terahertz camera for standoff security screening," *Appl. Opt.* **49**(19), E106–E120 (2010).
[9] Ahi, K., Shahbazmohamadi, S., and Asadizanjani, N., "Quality control and authentication of packaged integrated circuits using enhanced-spatial-resolution terahertz time-domain spectroscopy and imaging," *Optics and Lasers in Engineering* (2017, accepted).
[10] Ahi, K., "Mathematical modeling of thz point spread function and simulation of THz imaging systems," *IEEE Trans. Ter. Sci. Tech.* **7**6, 747–754 (2017).
[11] Jacobsen, R., Mittleman, D., and Nuss, M., "Chemical recognition of gases and gas mixtures with terahertz waves," *Opt. Lett.* **21**(24), 2011–2013 (1996).
[12] Zeitler, J., Taday, P., Newnham, D., Pepper, M., Gordon, K., and Rades, T., "Terahertz pulsed spectroscopy and imaging in the pharmaceutical setting - a review," *Journal of Pharmacy and Pharmacology* **59**(2), 209–223 (2007).
[13] Lo, Y. and Leonhardt, R., "Aspheric lenses for terahertz imaging," *Opt. Exp.* **16**(20), 15991–15998 (2008).
[14] Yang, X., Zhao, X., Yang, K., Liu, Y., Liu, Y., Fu, W., and Luo, Y., "Biomedical applications of terahertz spectroscopy and imaging," *Trends in Biotechnology* **34**(10), 810–824 (2016).
[15] Tuchin, V., [*Tissue Optics: Light Scattering Methods and Instruments for Medical Diagnostics, Third Edition*], SPIE Press (2015).
[16] Tuchin, V., "Tissue optics and photonics: Biological tissue structures," *Journal of Biomedical Photonics and Engineering* **1**(1), 3–21 (2015).
[17] Tuchin, V., "Tissue optics and photonics: Light-tissue interaction," *Journal of Biomedical Photonics and Engineering* **1**(2), 2469 (2015).
[18] Tuchin, V., "Tissue optics and photonics: Light-tissue interaction II," *Journal of Biomedical Photonics and Engineering* **2**(3), 030201 (2016).
[19] Lord Rayleigh, F. R. S., "XXXI. Investigations in optics, with special reference to the spectroscope," *Phil. Mag.* **8**(49), 261–274 (1879).
[20] Born, M. and Wolf, E., [*Principles of Optics (Sixth Edition)*], Pergamon (1980).
[21] Chernomyrdin, N., Frolov, M., Lebedev, S., Reshetov, I., Spektor, I., Tolstoguzov, V., Karasik, V., Khorokhorov, A., Koshelev, K., Schadko, A., Yurchenko, S., and Zaytsev, K., "Wide-aperture aspherical lens for high-resolution terahertz imaging," *Rev. Sci. Instrum.* **88**(1), 014703 (2017).
[22] Lukyanchuk, B., Paniagua-Dominguez, R., Minin, I., Minin, O., and Wang, Z., "Refractive index less than two: photonic nanojets yesterday, today and tomorrow," *Opt. Mat. Exp.* **7**(6), 1820–1847 (2017).
[23] Pimenov, A. and Loidl, A., "Focusing of millimeter-wave radiation beyond the Abbe barrier," *Appl. Phys. Lett.* **83**(20), 4122–4124 (2003).
[24] Chernomyrdin, N., Schadko, A., Lebedev, S., Tolstoguzov, V., Kurlov, V., Reshetov, I., Spektor, I., Skorobogatiy, M., Yurchenko, S., and Zaytsev, K., "Solid immersion terahertz imaging with sub-wavelength resolution," *Appl. Phys. Lett.* **110**(22), 221109 (2017).
[25] Pham, H., Hisatake, S., Minin, O., Nagatsuma, T., and Minin, I., "Enhancement of spatial resolution of terahertz imaging systems based on terajet generation by dielectric cube," *APL Phot.* **2**(5), 056106 (2017).
[26] Zhang, Y., Zhou, W., Wang, X., Cui, Y., and Sun, W., "Terahertz digital holography," *Strain* **44**(5), 380–385 (2008).
[27] Krozer, V., Loffler, T., Dall, J., Kusk, A., Eichhorn, F., Olsson, R. K., Buron, J. D., Jepsen, P. U., Zhurbenko, V., and Jensen, T., "Terahertz imaging systems with aperture synthesis techniques," *IEEE Trans. Microwave Theory and Tech.* **58**(7), 2027–2039 (2010).
[28] Choporova, Y., Knyazev, B., and Mitkov, M., "Classical holography in the terahertz range: Recording and reconstruction techniques," *IEEE Trans. Ter. Sci. Tech.* **5**(5), 836–844 (2015).
[29] Petrov, N., Kulya, M., Tsypkin, A., Bespalov, V., and Gorodetsky, A., "Application of terahertz pulse time-domain holography for phase imaging," *IEEE Trans. Ter. Sci. Tech.* **6**(3), 464–472 (2016).

[30] Kulya, M., Balbekin, N., Gredyuhina, I., Uspenskaya, M., Nechiporenko, A., and Petrov, N., "Computational terahertz imaging with dispersive objects," *J Modern Optics* **64**(13), 1283–1288 (2017).

[31] Hunsche, S., Koch, M., Brener, I., and Nuss, M., "THz near-field imaging," *Opt. Comm.* **150**(1–6), 22–26 (1998).

[32] Chen, H.-T., Kersting, R., and Cho, G., "Terahertz imaging with nanometer resolution," *Appl. Phys. Lett.* **83**(15), 3009–3011 (2003).

[33] Moon, K., Park, H., Kim, J., Do, Y., Lee, S., Lee, G., Kang, H., and Han, H., "Subsurface nanoimaging by broadband terahertz pulse near-field microscopy," *Nano Lett.* **15**(1), 549–552 (2015).

[34] Mitrofanov, O., Lee, M., Hsu, J. W. P., Pfeiffer, L. N., West, K. W., Wynn, J. D., and Federici, J. F., "Terahertz pulse propagation through small apertures," *Appl. Phys. Lett.* **79**(7), 907–909 (2001).

[35] Popovic, Z. and Grossman, E. N., "THz metrology and instrumentation," *IEEE Trans. Ter. Sci. Tech.* **1**(1), 133–144 (2011).

[36] Tseng, T.-F., Yang, S.-C., Shih, Y.-T., Tsai, Y.-F., Wang, T.-D., and Sun, C.-K., "Near-field sub-thz transmission-type image system for vessel imaging in vivo," *Opt. Exp.* **23**(19), 25058–25071 (2015).

[37] Komandin, G. A., Chuchupal, S. V., Lebedev, S. P., Goncharov, Y. G., Korolev, A. F., Porodinkov, O. E., Spektor, I. E., and Volkov, A. A., "BWO generators for terahertz dielectric measurements," *IEEE Trans. Ter. Sci. Tech.* **3**(4), 440–444 (2013).

[38] Golay, M., "Theoretical consideration in heat and infrared detection, with particular reference to the pneumatic detector," *Rev. Sci. Instrum.* **18**(5), 347–356 (1947).

[39] Nyquist, H., "Certain topics in telegraph transmission theory," *Trans. Amer. Inst. Electric. Eng.* **47**, 617–644 (April 1928).

[40] Wang, S., Guo, W., Huang, T.-Z., and Raskutti, G., "Image inpainting using reproducing kernel hilbert space and heaviside functions," *J Computational and Applied Mathematics* **311**, 551–564 (2017).

[41] Dean, P., Mitrofanov, O., Keeley, J., Kundu, I., Li, L., Linfield, E. H., and Davies, A. G., "Apertureless near-field terahertz imaging using the self-mixing effect in a quantum cascade laser," *Appl. Phys. Lett.* **108**(9), 091113 (2016).

[42] Ikushima, K., Sakuma, H., and Komiyama, S., "A highly sensitive scanning far-infrared microscope with quantum hall detectors," *Rev. Sci. Instrum.* **74**(9), 4209–4211 (2003).

[43] Gompf, B., Gerull, M., Muller, T., and Dressel, M., "THz-micro-spectroscopy with backward-wave oscillators," *Infr. Phys. Tech.* **49**(1–2), 128–132 (2006).

[44] Buron, J. D., Petersen, D. H., Boggild, P., Cooke, D. G., Hilke, M., Sun, J., Whiteway, E., Nielsen, P. F., Hansen, O., Yurgens, A., and Jepsen, P. U., "Graphene conductance uniformity mapping," *Nano Lett.* **12**(10), 5074–5081 (2012).

[45] Wallace, V., Fitzgerald, A., Shankar, S., Flanagan, N., Pye, R., Cluff, J., and Arnone, D., "Terahertz pulsed imaging of basal cell carcinoma ex vivo and in vivo," *Brit. J Dermat.* **152**(3), 424–432 (2004).

[46] Ashworth, P., Pickwell-MacPherson, E., Provenzano, E., Pinder, S., Purushotham, A., Pepper, M., and Wallace, V., "Terahertz pulsed spectroscopy of freshly excised human breast cancer," *Opt. Exp.* **17**(15), 12444–12454 (2009).

[47] Joseph, C., Patel, R., Neel, V., Giles, R., and Yaroslavsky, A., "Imaging of ex vivo nonmelanoma skin cancers in the optical and terahertz spectral regions. Optical and terahertz skin cancers imaging," *Journal of Biophotonics* **7**(5), 295–303 (2014).

[48] Zaytsev, K., Kudrin, K., Karasik, V., Reshetov, I., and Yurchenko, S., "In vivo terahertz spectroscopy of pigmentary skin nevi: Pilot study of non-invasive early diagnosis of dysplasia," *Appl. Phys. Lett.* **106**(5), 053702 (2015).

[49] Ji, Y., Oh, S., Kang, S.-G., Heo, J., Kim, S.-H., Choi, Y., Song, S., Son, H., Kim, S., Lee, J., Haam, S., Huh, Y., Chang, J., Joo, C., and Suh, J.-S., "Terahertz reflectometry imaging for low and high grade gliomas," *Sci. Rep.* **6**, 36040 (2016).